Polymer Chemistry

ROYAL SOCIETY OF CHEMISTRY

PAPER

View Article Online
View Journal | View Issue

Cite this: *Polym. Chem.*, 2022, **13**, 1997

Synthesis and molecular characterization of well-defined polyanion miktoarm star copolymers

Christos Pantazidis, [a] Stelios Andreou,[a] Georgia Nikolakakou,[b,c] Emmanouil Glynos *[b,d] and Georgios Sakellariou *[a]

Received 13th February 2022,
Accepted 9th March 2022

DOI: 10.1039/d2py00195k

rsc.li/polymers

Over the last year, the synthesis of polyanion copolymers has attracted considerable attention for their utilization in single-ion electrolytes in lithium battery applications. Morphology has a significant impact on the properties of such materials thus, reliable synthetic protocols are needed for different macromolecular architectures. In this work, we report the synthesis and molecular characterization of a number of novel miktoarm star copolymers consisting of poly(ethylene oxide), PEO, and poly(lithium 4-styrenesulfonyl trifluoromethylsulfonyl imide), PSTFSILi, arms and a poly(divinylbenzene), PDVB, core. Initially, a PEO–NMP macroinitiator was synthesized. The "arm-first" method, was employed to produce a PEO star with approximately 22 arms, $(PEO)_{22}$, with a spacious PDVB core, bearing active NMP initiation sites. Subsequent polymerization of the STFSIK monomer ("in–out" method), followed by ion exchange using LiCl, produced well-defined PEO/PSTFSILi miktoarm stars. By varying the polymerization conditions, a series of miktoarm stars with various PSTFSILi molecular weights and Li^+ molar ratios, $r = [Li^+]/[EO]$, were synthesized. A kinetic study on the polymerization of STFSIK on the PEO star core, was completed, to reveal well-controlled and "living" features. We show that the macromolecular architecture and the ratio r have a huge impact on the crystallization, the segmental dynamics, and ion-conductivity of the miktoarm star copolymers.

Introduction

Conventional polymer electrolytes that are made by mixing a Li salt with a polymer host that can dissociate and contact ions, are dual-ion conductors as both the cations and the anions are mobile and free to move in the presence of an electric field. Due to the strong complexation of the Li^+ with the polymer host, the diffusion coefficient of the counter anions is several times larger than that of the cations and only a small fraction of the overall ionic current is carried by Li^+, as can be defined by the Li^+ transference number, t_{Li^+}. As an example, in poly(ethylene oxide), PEO, based electrolytes, t_{Li^+} can be as low as 0.2 to 0.3 that results in deleterious effects such as polarization that can greatly increase cell resistance, slow the charge/discharge rates, limit cell lifetime, and promote fast dendrite growth when incorporated in lithium metal batteries. Hence developing new means and novel polyanion macromolecular systems for the synthesis of single-ion conductors holds the key for the realization of safe, high-energy lithium metal batteries.[1]

The main idea of single lithium-ion solid polymer electrolytes (SLI-SPEs), is that the counter anion of the lithium salt is anchored to a polymer chain and is immobilized, in contrast to the Li cation which can move freely within the polymer matrix, thus being the sole contributor to conductivity.[2] In the case of dual-ion conductors, t_{Li^+} has a theoretical maximum of 0.5, while for SLI-SPEs, t_{Li^+} may reach values close to unity. One of the most prominent candidates for SLI-SPEs, is trifluoromethane sulfonylimide ($-SO_2-N^{(-)}-SO_2-CF_3$) lithium salt (TFSILi), linked to a polystyrene-like macromolecule (PSTFSILi). This polymer was first synthesized by Armand and coworkers and consists of a rigid backbone similar to that of polystyrene (PS), with pendant TFSI anion groups.[3]

As it was recently reported, miktoarm star morphology, may offer a viable solution to the decoupling between the mechanical behavior and the ionic conductivity, leading to solid polymer electrolytes with high ionic conductivity at room temperature, $\sigma > 10^{-4}$ S cm^{-1}.[4–6] Furthermore, it is known for PEO segments, that star/branched morphology can suppress crystallization[7] and therefore, increase the volume of the amorphous phase which offers ion conduction. In addition, the

[a]*Department of Chemistry, National and Kapodistrian University of Athens, Panepistimiopolis Zografou, 15771 Athens, Greece. E-mail: gsakellariou@chem.uoa.gr*
[b]*Institute of Electronic Structure and Laser, Foundation for Research and Technology-Hellas, P.O. Box 1385, 71110 Heraklion, Crete GR, Greece. E-mail: eglynos@iesl.forth.gr*
[c]*Departement of Chemistry, University of Crete, Heraklion, 700 13 Heraklion, Crete, Greece*
[d]*Departement of Materials Science and Technology, University of Crete, 71003 Heraklion, Crete, Greece*

incorporated PSTFSILi segments may offer structural robustness combined with facile Li^+ disassociation due to the large surface area of interaction with the PEO arms. To the best of our knowledge, only one PEO/PSTFSILi miktoarm star has been reported so far, using a functionalized POSS nanoparticle as a core. This synthetic procedure, afforded a multimodal dispersity of miktoarm stars with a maximum of 8 arms while the reported ion conductivity was as low as about 10^{-14} S cm^{-1} at 60 °C.[8]

Herein, we report the synthesis and molecular characterization of a number of well-defined miktoarm single-ion star copolymers with a poly(divinylbenzene) (PDVB) cross-linked core, and PEO/PSTFSILi arms with various molecular weight of PSTFSILi. Linear PEO was converted to a nitroxide-mediated polymerization macroinitiator, PEO–NMP. Subsequently, the polymerization and cross-linking reaction of DVB monomer, produced a PEO star with PDVB core, in which the NMP initiator groups were active. Finally, the polymerization of potassium 4-styrenesulfonyl (trifluoromethylsulfonyl) imide (STFSIK) and its subsequent Li-ion exchange, yielded the miktoarm star (Scheme 1). Using the same synthetic protocol, we explored the kinetics of the NMP polymerization of STFSIK, from the core of the PEO star and we were able to produce a number of miktoarm stars with different lengths of the PSTFSILi arm and as a result, with a variety of r = $[Li^+]/[EO]$ ratios. As we show, the proposed synthetic approach offers new means to systematically control r, that significantly affect the ion conduction, allowing us to synthesize materials with an ionic conductivity with about 7 orders of magnitude larger than other miktoarm polyanion stars reported in the literature.[8]

This procedure, bypasses the need of a core functionalization prior to arm grafting, and also offers control on several aspects of the miktoarm star, such as the molecular weight and the weight fraction of the arms, along with star functionality. Also, the complex macromolecular architecture of the miktoarm stars, and the associated geometrical constrains have a significant effect on the degree of Li^+ and PEO complexation and corresponding segmental dynamics of the PEO/Li complexes. As a result, the miktoarms remain amorphous and the crystallization behavior of the PEO arm is suppressed. All these parameters should have a direct impact on the utilization of such systems in Li-ion batteries and we believe that much research will soon arise on the subject of single – lithium ion miktoarm stars.

Experimental section

Materials

N-tert-Butyl-*O*-[1-[4-(chloromethyl)phenyl]ethyl]-*N*-(2-methyl-1-enylpropyl)hydroxylamine (Merck), sodium hydride (Merck), 18-crown-6 ether (ACROS Organics), dichloromethane (Fisher Scientific), diethyl ether (Fisher Scientific), chloroform (Fisher Scientific), lithium chloride (Merck) and *n*-heptane (CARLO ERBA) were used as purchased. Poly (ethylene glycol) methyl ether (Merck) was freeze dried prior to being used. Tetrahydrofuran (CARLO ERBA), methanol (CARLO ERBA) and dimethylformamide (CARLO ERBA) were dried and distilled. Divinyl benzene (isomers assay 60%, Merck) was dried using CaH_2 and the polymerization inhibitors were removed using a prepacked column, for removing *tert*-butylcatechol (Merck). The synthesis of the Potassium 4-styrenesulfonyl (trifluoromethylsulfonyl) imide monomer (STFSIK) was similar to Armand's work.[3]

Characterization

Size exclusion chromatography (SEC) was used to determine the molecular weight distribution values, $Đ = M_w/M_n$ of the prepared samples. The analysis was performed using a system composed of a Waters 600 high-performance liquid chromatographic pump, Waters Ultrastyragel columns (HT-2, HT-4,

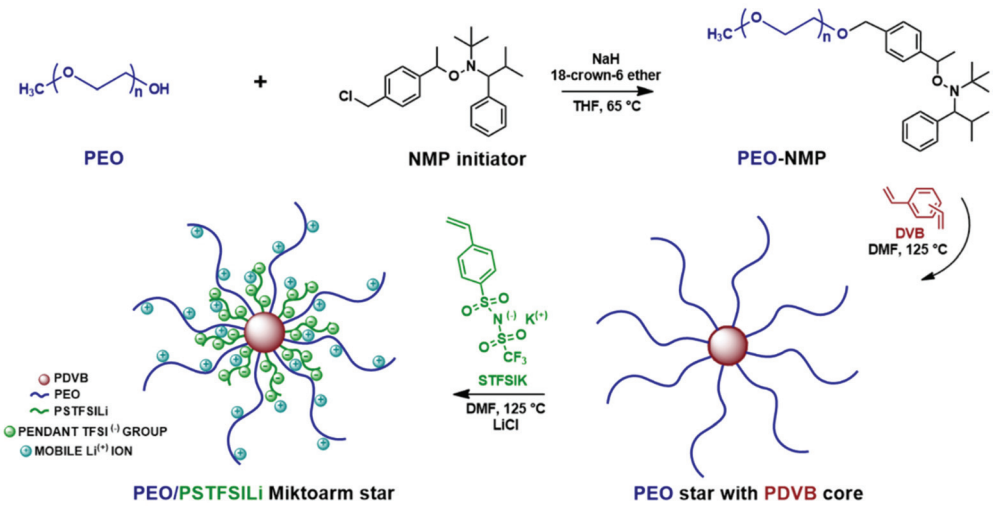

Scheme 1 Synthesis of a PEO/PSTFSILi miktoarm star with the "arm-first", "in–out" method.

HT-5E and HT-6E) and a Waters 410 differential refractometer. A 0.1 M LiBr in DMF solution was used as an eluent at a rate of 1 mL min^{-1}. The system was operated at 60 °C and PEO samples were used for its calibration.

Nuclear magnetic resonance (NMR) measurements were carried out on a 400 MHz Bruker Avance Neo instrument, using DMSO-d_6 as a solvent at 298 K.

The d*n*/d*c* value of the synthesized PEO star in methanol, was determined using a Chromatix KMX-16 differential refractometer at 25 °C (λ = 633 nm). Static light scattering measurements (SLS) were performed using BI-200SM Research Goniometer at 25 °C (λ = 640 nm).

The thermal properties of the single-ion miktoarm star copolymers were determined with a Discovery DSC 250 (TA Instruments) differential scanning calorimetry (DSC). The temperature range was from −110 °C to 130 °C.

The ionic conductivities of the synthesized macromolecules were measured inside an Argon glovebox using a Bio-Logic SP300 potentiostat and a homemade test cell, composed of a cylindrical Kentron 1000 PEEK (Mitsubishi Chemical Advanced Materials) spacer with 4 mm diameter and 2 mm thickness and blocking stainless steel electrodes. The ionic conductivity was determined from impedance spectroscopy where a sinusoidal voltage of 50 mV was applied from 7 MHz to 1 Hz. The ionic conductivity, σ, was estimated as:

$$\sigma = \frac{L}{RA}$$

where L is the electrolyte thickness and A is the area of contact and R the bulk resistance of the electrolyte taken at the plateau value in the Bode plot of the complex impedance *vs*. frequency. The estimated ionic conductivities were the same as those estimated by the Nyquist plots. The test cells were placed in a custom-made temperature chamber and studied at selective temperatures from 130 to 30 °C, in 10 °C steps during cooling. The samples had an equilibrium time of 30 min at each temperature.

PEO–NMP macroinitiator

The PEO–NMP macroinitiator was synthesized *via* reaction of poly(ethylene glycol) methyl ether (M_n = 4.6 kDa, $Đ$ = 1.03) with *N*-*tert*-butyl-*O*-[1-[4-(chloromethyl)phenyl]ethyl]-*N*-(2-methyl-1-phenylpropyl) hydroxylamine (NMP initiator) in the presence of NaH and 18-crown-6 ether (Scheme 1). The synthetic procedure was similar to that in Hawker's work[9] with slight modifications, mostly concerning the purification process. PEO (2.35 g, 5×10^{-4} mol, 1 eq.), NaH (50 mg, 2×10^{-3} mol, 4 eq.) and a small amount of 18-crown-6 ether (10 mg, cat.) were added to a Schlenk apparatus. Dry tetrahydrofuran (THF) was distilled in the apparatus and the contents were left to completely solubilize under nitrogen flow. After complete dissolution, and when the initial bubbling stopped, the NMP initiator (374 mg, 10^{-3} mol, 2 eq.) was added to the mixture and the apparatus was placed in a 65 °C oil bath in reflux conditions. The reaction was left for 20 h until completion, under constant nitrogen flow. Finally, a few drops of water were added to neutralize excess NaH, and the solvent was removed. Dichloromethane was used to solubilize the PEO–NMP and the macroinitiator was precipitated in a large excess of diethyl-ether, and subsequent washes were employed to completely remove the excess of the NMP initiator. To ensure that there were no NaOH impurities left in the sample, the solvents were removed and the sample was dissolved in water and placed in a dialysis membrane with 1 kDa MWCO. Dialysis was employed against deionized water and finally the purified macroinitiator was obtained after freeze drying (2.45 g, 96.5% yield).

PEO star with PDVB crosslinked core

To produce the PEO star, 1 g of the PEO–NMP (2×10^{-4} mol, 1 eq.) was placed in a Schlenk flask along with 332 μL (299 mg, 2 3 × 10^{-3} mol, 11.5 eq.) of DVB monomer mixture and 3 mL of distilled dimethylformamide (DMF). The apparatus was connected to a high vacuum line and degassed through 4 freeze–pump–thaw cycles. The flask was closed, disconnected from the vacuum line and placed in an oil bath of 125 °C for 4 h under high vacuum. To pause the polymerization reaction, the apparatus was removed from the oil bath and quenched in cold running water for a few minutes. At this point, the solution was highly viscous due to the formation of the crosslinked polymers. Size exclusion chromatography revealed the formation of a multimodal distribution of star polymers along with unreacted PEO arm and its dimer. The solvent, along with the unreacted DVB, were removed in the vacuum line, and the crude product was dissolved in 50 mL of chloroform (2% w/v). The solution was slightly cloudy, probably due to the fact of a small amount of PDVB conjugates, which were removed by filtration. Fractional precipitation was carried out on the filtrate, in order to purify the PEO star polymer, using heptane as a non-solvent to afford 380 mg (30% yield) of a well-defined monodispersed PEO star with a PDVB crosslinked core (Fig. 2).

Polymerization of STFSIK from the core of the PEO star

PEO star (50 mg) was added to a Schlenk tube together with STFSIK monomer (100 mg) and 0.5 mL of distilled DMF. As in the previous procedure, the solution was degassed, and the polymerization took place under high vacuum at 125 °C. Finally, the tube was placed under cold running water to stop the ongoing propagation. The DMF was removed, and the crude product containing the produced miktoarm star, along with unreacted STFSIK was dissolved in dimethyl sulfoxide (DMSO). The solution was placed in a dialysis membrane with a MWCO of 12–14 kDa and dialysis against a LiCl aqueous solution was employed, followed by dialysis against deionized water to remove the salt excess. In this manner, we were able to completely purify the polymer from any unreacted monomer and subsequently perform the ion-exchange from the potassium form to the lithium one. After the purification process, the PEO/PSTFSILi miktoarm star was freeze dried prior to characterization. To explore the kinetics of the STFSIK polymerization from the PDVB core of the synthesized PEO

star (Scheme 1), five samples were prepared following the same procedure, while only the time of the polymerization varied from 10 min to 120 min.

Results and discussion

PEO–NMP macroinitiator

For the preparation of the macroinitiator, a Williamson reaction took place between the hydroxyl group at the end of the PEO chain and an NMP initiator with a TIPNO persistent radical (Scheme 1). ^{1}H NMR was employed to assess the purity of the product and the fact that each PEO chain, bore the NMP initiator group after the reaction (Fig. 1a). Integration of the phenyl group protons (δ: 7.5–7.1 ppm) compared to the protons of the PEO backbone (δ: 3.73–3.41 ppm) gave the average number of EO monomeric units (105 units) per chain, which coincided with the initial PEO. In the same manner, the weight composition of PEO and NMP initiator were extrapolated. The average molecular weight estimation of the macroinitiator, taking in account the additional molecular weight of the NMP initiator unit, was approximately 5 kDa.

PEO star with PDVB crosslinked core

Controlled/"living" radical polymerization techniques have been successfully employed to produce star polymers with a variety of different procedures and chemical compositions.[10,11] For our synthetic approach, we chose to use the nitroxide-mediated polymerization for a variety of reasons. NMP, is a facile and well-controlled procedure with all the aspects of a "living polymerization". Since the use of a metal catalyst is not required, NMP produces polymers with no additional metal residue, important for materials designed for battery applications.

Specifically, a PEO–NMP macroinitiator was used to polymerize a bifunctional monomer mixture (DVB) under high vacuum in DMF solution, to afford a PEO star with PDVB cross-linked core with active NMP polymerization sites, which were later used for subsequent polymerization of STFSIK monomer. This synthetic strategy, is referred to as an "arm-first", "in–out" method, for the miktoarm star synthesis. The PEO–NMP macroinitiator bore a TIPNO group at the end of the chain, which generally offers high polymerization control for styrene-like monomers. Additionally, in our previous work, we have shown that the TIPNO radical yielded exceptional results for the "living polymerization" of the STFSIK monomer.[12] The DVB mixture, consisted of *meta* and *para* isomers (60%) of divinylbenzene which can be polymerized and cross-linked, and ethyl vinylbenzene (40%), which can be polymerized, but due to the absence of a second vinyl group, does not take part in the cross-linking process. We chose to employ this DVB mixture, in order to produce a large and generally spacious PDVB core to facilitate the initiation of the sequential polymerization of the STFSIK monomer.

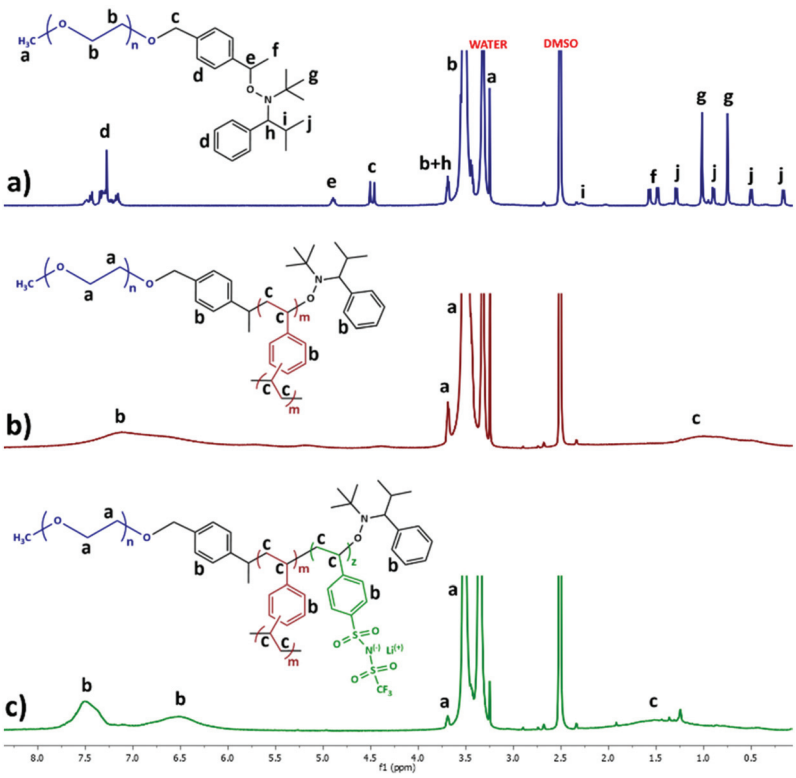

Fig. 1 ^{1}H NMR in DMSO-d6 spectra of the synthesized PEO macroinitiator (a), PEO star with PDVB core (b), and PEO/PSTFSILi miktoarm star copolymer (c).

As a result of the polymerization and cross-linking reaction of the DVB bifunctional monomer, a multimodal molecular weight distribution was initially obtained from which, the purified PEO star product was isolated through fractional precipitation. Size exclusion chromatography revealed a well-defined and monomodal molecular weight distribution (Fig. 2). Prior to the polymerization of STFSIK, the sample was characterized in terms of molecular weight, and composition.

To determine the dn/dc value of the sample, two solutions (C_1: 6.5 mg mL^{-1}, C_2: 3.1 mg mL^{-1}) of the synthesized PEO star in dry MeOH were prepared, and the dn/dc value was found to be 0.159 mL g^{-1} at 25 °C. The molecular weight M_w was extrapolated *via* static light scattering measurements (SLS). Dilute solutions (C_1: 5.09 g mL^{-1}, C_2: 3.05 g mL^{-1}, C_3: 2.08 g mL^{-1}, C_4: 1.29 g mL^{-1}) of the PEO star in dry methanol were measured in various angles ranging from 135° to 40° for the Zimm Plot to be constructed. The previously found dn/dc value of the sample was employed, and the molecular weight was calculated to be 127 kDa. ^{1}H NMR (Fig. 1b) was used to calculate the various mass compositions (wt%), using the integration of the broad peak that corresponds to the aromatic protons of the core (δ: 8.0–6.0 ppm) and the broad peak that corresponds to the aliphatic protons of the PEO chain (δ: 3.73–3.41 ppm). Combining the results of the molecular characterization, we were able to determine that the average number of PEO arms in the synthesized star is approximately 22. The results are summarized in Table 1.

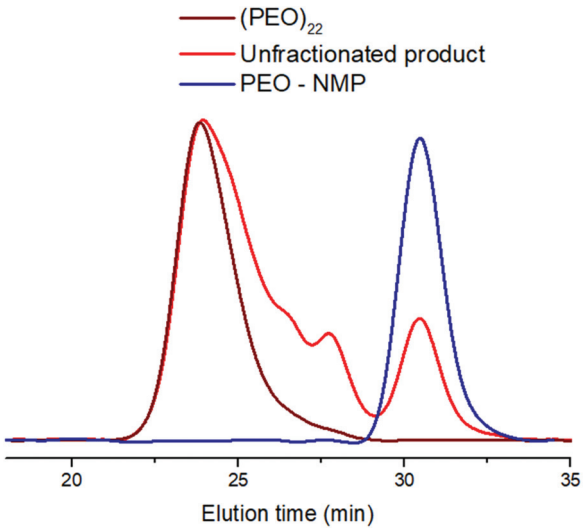

Fig. 2 SEC eluograms, comparing the PEO–NMP, the crude unfractionated product of the cross-linking reaction with DVB and the fractionated star product, $(PEO)_{22}$.

Kinetic study of the STFSIK polymerization

A $(PEO)_{22}$ star was used as a macroinitiator with multiple active sites on its PDVB core to polymerize STFSIK, followed by an ion-exchange reaction to produce the lithiated product (Scheme 1). The polymerization of STFSIK took place in DMF, under high vacuum, and the subsequent purification of the miktoarm star from any unreacted monomer, was realized through dialysis with an aqueous solution of LiCl to achieve the Li-ion exchange and subsequent dialysis with deionized water. To confirm that the polymerization of the STFSIK monomer proceeded in a controlled manner, all samples were prepared with the same experimental protocol and the sole variable throughout the procedure, was the time of polymerization reaction, ranging from 10 to 120 min. The initiator/monomer ratio was kept constant, using an initial initiator concentration of $[I]_0 = 8.57 \times 10^{-3}$ mol L^{-1}.

According to the feed ratio of STFSIK monomer, a theoretical total monomer conversion would yield approximately 32 monomeric units of STFSILi per 105 units of EO in the final polymer [Abbreviated: MIKTOARM STAR, PEO (105) _PSTFSILi (32)]. The estimation of monomer conversion was realized through ^{1}H NMR spectroscopy in DMSO-d_6, using the spectra

Table 1 Molecular characteristics of the synthesized samples

Sample name[a]	Time of STFSIK polymerization reaction	M_n (kDa)	$Đ^d$ (M_w/M_n)	PEO wt. % [b]	PSTFSILi		PDVB wt. % [b]	NMP in. wt.% [b]	r ([Li$^+$]/[EO] [b]
					wt.% [b]	Monomer conversion[b]			
PEO–NMP	—	5 [b]	1.03	93.2	—	—	—	6.8	—
$(PEO)_{22}$	—	127 [c]	1.19	79.8	—	—	14.4	5.8	—
MIKTOARM STAR, PEO (105) _PSTFSILi (4.8)	10 min	160 [b]	1.25	62.9	21.2	15.6%	11.3	4.6	0.046
MIKTOARM STAR, PEO (105) _PSTFSILi (9.9)	20 min	198 [b]	1.24	51.3	35.7	31.3%	9.2	3.8	0.095
MIKTOARM STAR, PEO (105) _PSTFSILi (14.4)	40 min	228 [b]	1.26	44.4	44.4	43.8%	8.0	3.2	0.137
MIKTOARM STAR, PEO (105) _PSTFSILi (17.9)	60 min	254 [b]	1.26	40.0	49.9	56.3%	7.2	2.9	0.171
MIKTOARM STAR, PEO (105) _PSTFSILi (21.4)	120 min	299 [b]	1.24	36.9	54.9	65.6%	5.5	2.7	0.204

[a] The abbreviations for the miktoarm stars show the ratio between EO and STFSILi units. 105, is the average number of EO units per PEO arm so we chose to use this as a reference. [b] Calculated from ^{1}H NMR in DMSO-d_6. [c] Extrapolated from Zimm Plot diagram of SLS. [d] Taken from SEC, calibrated with PEO standards.

of the final, lithiated form of each miktoarm star (Fig. 1c). We were able to calculate the molar ratio of the PSTFSILi and PEO in the produced miktoarm stars through the integration of the phenyl group protons (δ: 8.0–6.0 ppm) compared to the protons of the PEO backbone (δ: 3.73–3.41 ppm). For the calculations of PSTFSILi, the integration that corresponded to the NMP initiator and the PDVB core (Fig. 1b), was subtracted, since all the phenyl group peaks appear in the same ppm region. Thus, we were able to extrapolate the monomer conversion in each polymerization. The same integrations, were used to calculate the various mass compositions of each component in the final purified samples (Table 1).

The monomer conversion *vs.* reaction time plot (Fig. 3a) exhibits a non-linear behavior, which is expected in such radical polymerizations. At lower times of reaction and therefore lower monomer conversion values, a somewhat linear behavior of the plot line is observed which is later discontinued at higher conversion values. This happens probably, due to the constantly increasing viscosity of the polymerization solution, paired with the decreasing monomer concentration.

The molecular weight (M_w) of the PEO star that was used as a macroinitiator, was known through SLS measurements and the total molecular weight of the PEO/PSTFSILi miktoarm stars was calculated using the mass compositions that ^{1}H NMR spectroscopy yielded. Size exclusion chromatography revealed an overall well-controlled radical polymerization of the STFSIK monomer indicated by the complete shift of the eluograms to lower elution volumes, according to the reaction time (Fig. 4). The linearity of the M_n *vs.* monomer conversion plot (Fig. 3b), showed the controlled propagation of the polymerization reaction, and that, combined with the low molecular weight distributions that were obtained using SEC, revealed the production of well-defined miktoarm stars in each case.

As it has already been shown by multiple experimental data, the "living" nature of a controlled, radical polymerization is, in many cases, governed by the Persistent Radical Effect, PRE.[13] This effect, occurs in the early stages of radical polymerizations, in which a persistent radical is being used to provide control over chain propagation. In the case of NMP, the initiation of the polymerization occurs with the homolysis of the initiator, RN, to produce a transient [R*] and a nitroxide radical [N*]. At low monomer conversions, transient radicals may react to produce irreversibly terminated molecules and thus a built up of persistent radicals [N*], resulting in a more controlled reaction. In particular, Matyjaszewski *et al.* showed the important role of PRE, using computer simulations.[14] Taking that effect under consideration, in the case of an NMP reaction that exhibits the features of a "living" polymerization, eqn (1) yields the mathematical correlation of the ln([M_0]/[M]) to the initial concentration of the initiator and to the reaction time.

$$\ln\frac{[M_0]}{[M]} = \left(\frac{3}{2}k_p\right)(k[RN]_0/3k_t)^{1/3}(t)^{2/3} \quad (1)$$

In this expression, [M_0] refers to the initial monomer concentration and [M] refers to the concentration of monomer that has remained unreacted, at any given time (t). The constant k, is the ratio of the rate of decomposition to the rate of

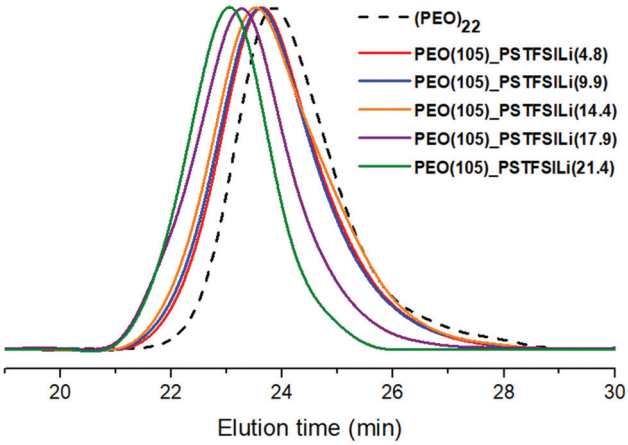

Fig. 4 Comparative eluograms of the $(PEO)_{22}$ macroinitiator star and the miktoarm stars synthesized with different reaction times.

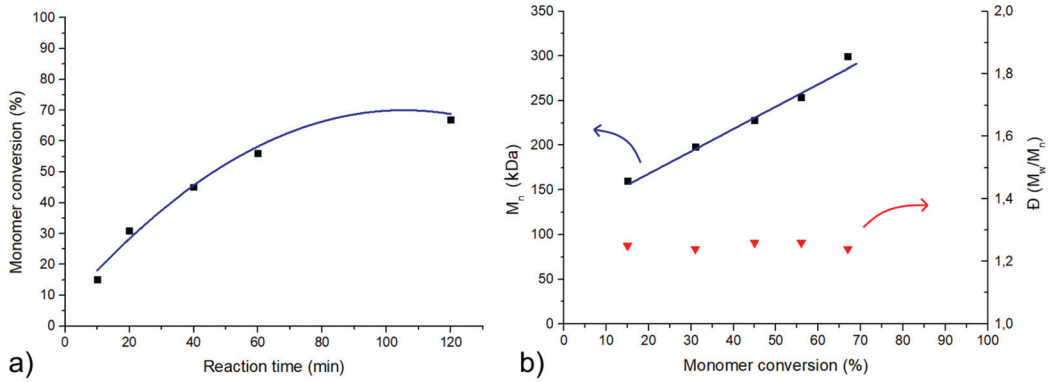

Fig. 3 (a) Monomer conversion *vs.* reaction time for the STFSIK polymerization on a $(PEO)_{22}$ star with PDVB core. (b) Molecular weight of the purified miktoarm stars *vs.* monomer conversion and molecular weight distribution. The blue lines are guide lines to the eyes.

the combination constant (k_d/k_c) that occurs between the transient [R*] and the persistent nitroxide radical [N*]. Respectively, k_t is the rate constant of the irreversible termination between two transient radicals. In the polymerizations where the experimental conditions offer a "living" system with minimal irreversible terminations, the concentration of radicals is constant at any given moment and in very close approximation to the initial initiator concentration $[RN]_0$.

That being said, if the termination reactions are kept to a minimum, plotting the $\ln([M_0]/[M])$ *vs.* $t^{2/3}$ (reaction time$^{2/3}$) should exhibit a linear fit, while the plot line of $\ln([M_0]/[M])$ *vs.* t (reaction time) should show a downward curvature.[15] The plot lines of our experimental data are presented in Fig. 5, and the linearity of the $\ln([M_0]/[M])$ *vs.* $t^{2/3}$ plot, reveals that the termination reactions were negligible throughout the polymerization reaction. As expected from eqn (1), the $\ln([M_0]/[M])$ *vs.* t plot, shows a downward curvature. The combination of the kinetic study findings, reveal an overall well-controlled polymerization of the STFSIK monomer, from the core of the $(PEO)_{22}$ star.

As revealed in Table 1, the initial PEO star consisted of an average of 22 arms. Considering the synthetic route that we followed, the PDVB core of each star, should theoretically bear the same number of initiation sites, thus yielding the same average number of arms for the polymerization of the second monomer $[(PEO)_x(PSTFSILi)_y$ where $x \approx y \approx 22]$. However, in reality, when producing miktoarm stars with the "arm-first", "in–out" method, the number of arms produced by the second polymerization is always lower, due to a number of factors such as the size of the core, the general steric hindrance and possible irreversible termination reactions. In our case, we used purified materials and high vacuum techniques that generally produce polymers with extremely high-end fidelity, to eliminate the possibility of unwanted terminations, combined with the fact that the $(PEO)_{22}$ star that we used as a multi-site macroinitiator, had a spacious PDVB core to avoid steric hindrance. We acknowledge the fact that the PSTFSILi average number of arms may be slightly lower than that of the PEO, but we believe that the theoretical maximum of 22, is also a close approximation for the number of the PSTFSILi arms. In any case, the main focus of the synthetic protocol on this kinetic study is the controlled polymerization of the STFSIK monomer from the core of the PEO star, combined with the ability to have control over the $[Li^+]/[EO]$ ratio.

Thermal properties

The differential scanning calorimetry data for the linear PEO arm precursor and the $(PEO)_{22}$ star with PDVB core during cooling and heating are shown in Fig. 6a and b with black and red lines, respectively. While both the linear PEO precursor and the $(PEO)_{22}$ star show an exothermic peak during cooling and the corresponding endothermic melting during heating due to the crystallization of PEO, the architecture has a significant effect on the degree of crystallization. For the linear PEO, the degree of crystallinity is found to be 89.7%, while for the $(PEO)_{22}$ the degree of crystallinity is significantly lower, at 55.9%, indicating that branching and associated geometrical constrains significantly affected the crystallization behavior of PEO, as it is known for branched polymers.[8,16,17] The apparent crystallization temperature of the $(PEO)_{22}$ star during the non-isothermal crystallization at a cooling rate of 10 °C min^{-1} is lower than that of the linear PEO precursor, (red and black lines in Fig. 6a, respectively). This may be explained by the lower crystallization rate of PEO stars compared to their linear analogues[18] and the effect of macromolecular architecture and associated geometrical constrains on the non-equilibrium nature of the folded PEO chains.[19]

For the miktoarm star with the largest STFSILi molar ratio synthesized in this study, *i.e.*, for $r = [Li^+]/[EO] = 0.204$, the miktroarms remained amorphous and the crystallization behavior of the PEO arm was completely suppressed; no endothermic peak was seen during the first heating, nor for subsequent cooling and heating scans with the DSC (Fig. 6). This behavior remained with decreasing r, and in particular the crystallization of PEO was completely suppressed for r = 0.171, 0.137 and 0.095. Noticeable, our data indicate a profound effect of the star-shaped architecture on the crystallization behavior of PEO/PSTFSILi polyanion macromolecules. In particular, Balsara and coworkers, showed that linear PEO-*b*-PSTFSILi block copolymers, with a similar M_w of the PEO

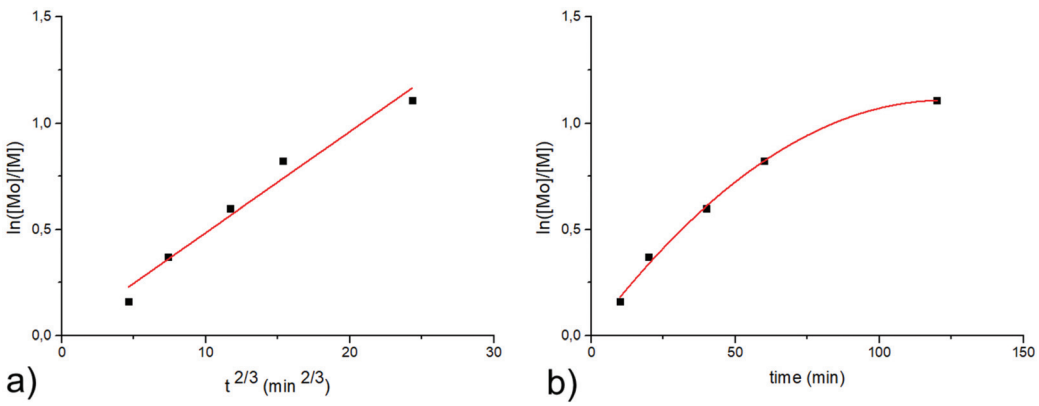

Fig. 5 Plot lines of $\ln([M_0]/[M])$ *vs.* $t^{2/3}$, and *vs.* t (reaction time) at a and b, respectively. The red lines are guide line to the eyes.

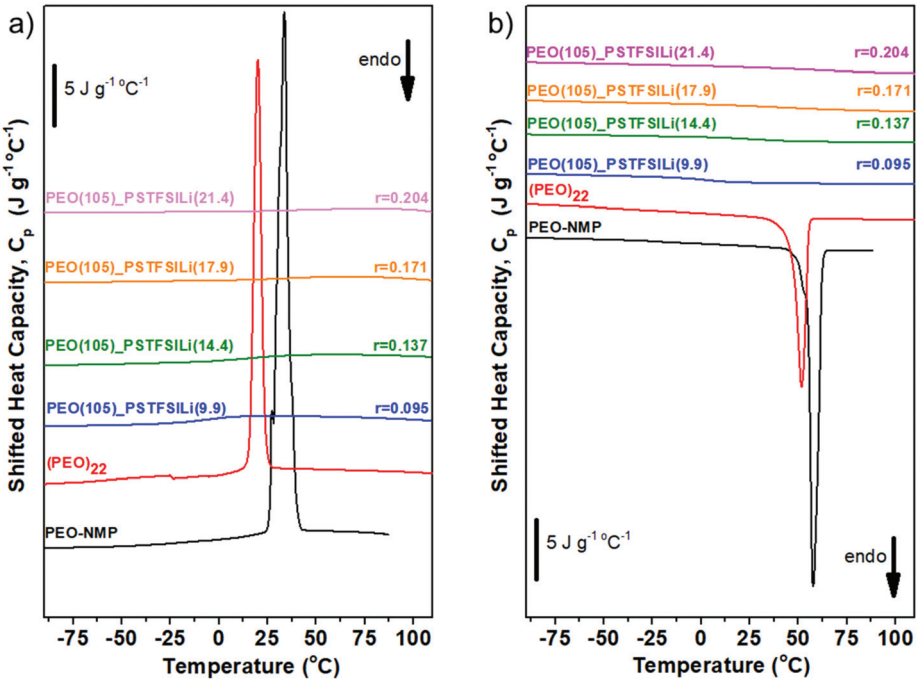

Fig. 6 Cooling (a) and heating (b) DSC thermographs of the linear PEO–NMP (arm precursor, black lines), the $(PEO)_{22}$ star with PDVB core (red lines) and the PEO/PSTFSILi miktoarm stars with r = [Li^+]/[EO] = 0.096 (blue lines), 0.137 (green lines), 0.171 (orange lines), and 0.204 (magenta lines). The data are shifted vertically for clarity while the black vertical bar indicates a scale of 5 J g^{-1} C^{-1} in heat capacity.

block as the PEO arms in this study, remained amorphous for M_w of PSTFSILi that resulted to a r = 0.150 or larger;[20] *i.e.*, more than two times larger than that of what we report for the star-shaped PEO/PSTFSILi copolymers. The crystallization behavior of PEO-*b*-PSTFSILi was discussed in terms of the low degree of ion-dissociation, as the result of the microphase separation of the PEO and PSTFSILi blocks; *i.e.*, Li^+ ions are trapped in the PSTFSILi-rich phase reducing the effective Li^+ density in the PEO rich phase. In our case, the utilization of the miktoarm architecture, significantly increases the PEO/PSTFSILi contacts, and along with the geometrical constrains impose by the macromolecular architecture, lead to amorphous materials even at a [Li^+]/[EO] ratio close to 0.046.

The situation becomes rather complex for the miktoarm star with the lower STFSILi molar ratio synthesized in this study, *i.e.*, for r = [Li^+]/[EO] = 0.046. While an endothermic peak was observed in the first heating from room temperature (black solid line in Fig. 7), no crystallization or melting was observed during the subsequent cooling and the next heating (dashed blue line and solid blue line in Fig. 7, respectively). These data indicate that the presence of the PSTFSILi arms, and the corresponding complexation of the Li^+ with the EO significantly affects/suppresses the crystallization behavior of PEO, similar to the behavior known for PEO/LiTFSI-based electrolytes.[6,21] The data in Fig. 7 indicate that for r = 0.046 the crystallization behavior is governed by very slow crystallization kinetics in the miktoarm copolymer (arrested crystallization kinetics) as upon melting the material can't crystallize within the normal DSC measurement conditions; cooling rates as

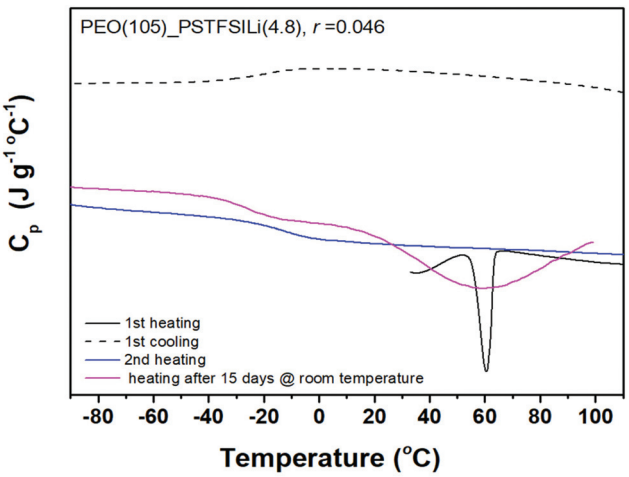

Fig. 7 DSC traces for the PEO(105)_PSTFSILi(4.8) miktoarm star, with r = 0.046. During first heating (black line), during first cooling (black dashed line) and during second heating at 10 °C min^{-1} (blue line). The magenta line corresponds to the DSC trace during heating after the sample was left for 15 days at room temperature in an inert environment. The data are shifted vertically for clarity.

slow as 1 °C min^{-1} were used but no crystallization was observed. Notably, when the sample was left for 15 days in an inert atmosphere at room temperature, it was partially crystallized (a very broad endothermic peak was observed during heating in the DSC scan, magenta line in Fig. 7) but its crystallization state was far from what was seen in the as-made sample (black line in Fig. 7).

Fig. 8 plots the T_g of the PEO as a function of r (black solid squares) along with the data from Balsara group on linear PEO-*b*-PSTFSILi block copolymers (open red cycles).[20,22] It is important to point out that the linear PEO-*b*-PSTFSILi molecules had a very similar M_w of the PEO block with the reported polyanion miktoarm stars. Noticeably the T_g of PEO arms in the PEO/PSTFSILi miktoarm star copolymers significantly increases with r, in a roughly linear fashion, reaching a value of around 60 °C for r = 0.204. This behavior is considerably different to that of the corresponding linear PEO-*b*-PSTFSILi block copolymers; the T_g increasing significantly less with r, converging to a value of around −20 °C for r >0.190. The fact that the crystallization of the PEO arms was fully suppressed for r >0.046, along with the large T_g enhancement of the PEO with r, indicates a strong Li^+/EO complexation that may be rationalized in terms of the resulted macromolecular morphology of the proposed systems. In particular, the reported polyanionic miktoarm stars could be considered as core/shell structures with the core region composed of PSTFSILi and PEO segments while the shell is composed by the longer, crystallizable, PEO arm; even at r = 0.204, the PEO arms are significantly longer than the PSTFSILi arms (about 21 monomeric units of STFSILi *versus* 105 monomers of EO). The presence of both PEO and PSTFSILi segments at the core region ensured the efficient Li^+ dissociation, that is located primarily at the PEO rich shell region, separated from the $TFSI^-$ at the core region. The latter, along with the dynamical slowdown of star-shaped polymers compared to their linear analogues, associated with the increased density and constrained dynamics close to the core regions,[23–25] results in T_g values that are significantly larger than their linear diblock analogues (Fig. 8).

Fig. 9 reports the ion conductivity as a function of temperature for the miktoarm stars synthesized in this study. It is important to point out that the sample with the highest $[Li^+]$/[EO] ratio [PEO(105)_PSTFSILi(21.4), r = 0.204] was very brittle and hard to handle so it couldn't be properly shaped for the impedance spectroscopy measurements. Our data show that ionic conductivity monotonically increases with decreasing the length of the PSTFSILi arms. This may be attributed to the strong increase of T_g (or a significant decrease of PEO segmental dynamics) with increasing PSTFSILi content. Noticeably, our synthetic approach and corresponding macromolecular characteristics of the synthesized PEO/PSTFSILi star-shaped copolymers, significantly affected the ionic conductivity of the resulted single-ion by design electrolytes. In particular, the best performing, PEO(105)_PSTFSILi(4.8), star-shaped copolymer exhibited about 7 order of magnitudes larger ionic conductivity than what was reported in the case of miktoarm stars PEO/PSTFSILi where a POSS nanoparticle was used as a core (Saito *et al.*).[8] To the best of our knowledge, the system of Saito *et al.* is the only other PEO/PSTFSILi star shaped copolymer reported in the literature. The large difference in conductivity may be attributed to the fact that PEO(105) _PSTFSILi(4.8) has PEO arms that are significantly longer than the PSTFSILi arms providing both a larger volume of the ion-conducting PEO phase, but also a highly interconnected, with low tortuosity PEO phase.

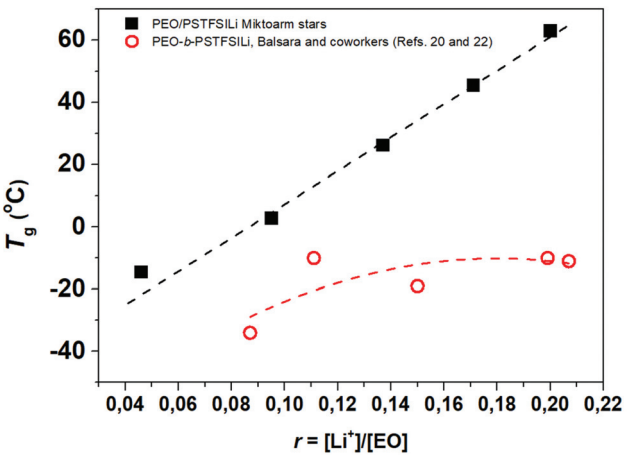

Fig. 8 Glass Transition temperature of PEO as a function of salt concentration for the PEO/PSTFSILi miktoarm stars (black solid squares) and linear PEO-*b*-PSTFSILi diblock copolymers (data taken from ref. 20 and 22).

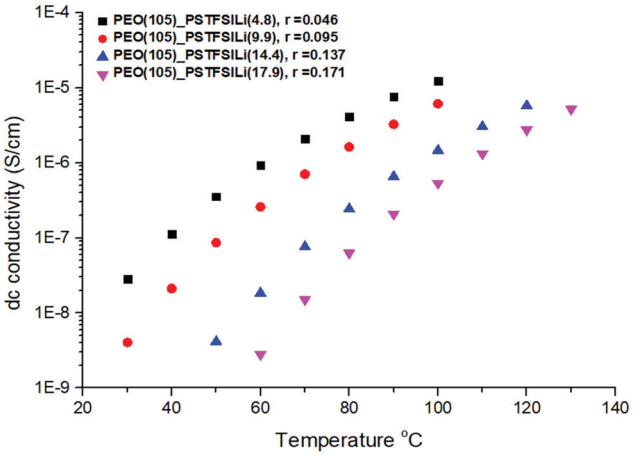

Fig. 9 Ionic conductivity *vs.* temperature plots, for the synthesized miktoarm star copolymers.

Our data indicate that the dependence of ion conductivity on r in the polyanionic miktoarm stars is much more complex than that in regular polymer electrolytes composed of blends of linear PEO with LiTFSI. In particular, in linear PEO/LiTFSI blends the ionic conductivity has a non-monotonic behavior *versus* r due to two competed factors: on one hand, ionic conductivity increases with r as the free ion concentration increases, and on the other hand polymer dynamics decrease monotonically with increasing r that tends to decrease ion conductivity (ion motion/transport is coupled with segmental dynamics). For PEO with M_w >2 kg mol^{-1} maximum in ionic conductivity has been reported to be at about r ~0.08.[6] In our case, the situation is rather more complex as r increases with increasing the length of PSTFSILi arms that also decrease the volume fraction of the conductive PEO phase that tend to

decrease conductivity. This, along with the strong T_g enhancement with r (much stronger than in the corresponding linear PEO/LiTFSI blends) results in a monotonic increase of conductivity with decreasing r even at values as low as 0.046. The conductivity will eventually reach a maximum for lower values of r, as the concentration of free ions will dramatically decreases, but experimentally the synthesis of such macromolecule is very challenging with certain limitations. We should also note that the miktoarm star with r = 0.046 has an average of 4–5 STFSILi monomeric units per arm, given that the polymerization was propagated from all the 22 initiation sites. Furtherly, we did try to synthesized polyanionic miktoarm stars with lower r but solubility issues in such systems prohibited the synthesis of final lithiated form with the same experimental protocol (water dialysis). It is important to point out that the synthetic protocol reported here allows the synthesis of well-defined polyanion miktoarm star copolymers, with tunable/controlled macromolecular characteristics (*i.e.*, number of arms, wt% of PEO and or PSTFSILi/r = [Li^+]/[EO]), that may hold the key for the design of single-ion solid polymer electrolytes with unpresented properties.

Conclusions

In conclusion, we report the successful synthesis and purification of a PEO-NMP macroinitiator, followed by the polymerization and cross-linking reaction of the DVB monomer to produce a $(PEO)_{22}$ star with PDVB core. The active initiation sites of the PDVB core were used for the subsequent polymerization of STFSIK which, through Li-ion exchange using LiCl, finally afforded the PEO/PSTFSILi miktoarm stars. The kinetic study of the STFSIK polymerization from the core of the PEO star, using active NMP initiation sites, revealed a well-controlled polymerization with "living" features, reaching high monomer conversion (~65%). All synthesized samples yielded well-defined, monomodal molecular weight distributions in size exclusion chromatography.

With this approach, we introduce synthetic protocols for such miktoarm stars of PEO/PSTFSILi, with control over several aspects of the procedure, such as the molecular weight of the PEO arms and the amount of DVB added, the combination of which, impacts the size and functionality of the star polymer. Also, the weight fraction of PSTFSILi can be controlled, thus providing the r = [Li^+]/[EO] molar ratio, important for conductivity studies. Additionally, the complex macromolecular architecture of the miktoarm stars, and the associated geometrical constrains have a significant effect on the degree of Li^+ and PEO complexation and corresponding segmental dynamic of the PEO/Li complexes. As a result, except from the lower r of 0.046 synthesized in this study, the miktroarms remain amorphous and the crystallization behavior of the PEO arm is completely suppressed, while the T_g of PEO arms in the miktoarm star copolymers significantly increases with r. Noticeably, the remarkable ability to systematically control the macromolecular characteristics of the reported miktoarm stars of PEO/PSTFSILi allowed us to synthesize single-ion electrolytes with an ionic conductivity that is about 7 order of magnitudes higher compared to other reported PEO/PSTFSILi miktoarm systems.[8] A systematic correlation of the macromolecular characteristics, namely functionality and M_w of the PEO and PSTFSILi arms, on the ionic conductivity – mechanical property relation of the resulted single-ion electrolytes, is part of our ongoing work.

Conflicts of interest

There are no conflicts to declare.

Acknowledgements

This research has been co-financed by the European Union and Greek National funds through the Operational Program Competitiveness and Innovation, under the call RESEARCH – CREATE – INNOVATE (project code: T1EΔK-02576).

References

1 L. Long, S. Wang, M. Xiao and Y. Meng, Polymer electrolytes for lithium polymer batteries, *J. Mater. Chem. A*, 2016, **4**, 10038–10069.
2 H. Zhang, C. Li, M. Piszcz, E. Coya, T. Rojo, L. M. Rodriguez-Martinez, M. Armand and Z. Zhou, Single lithium-ion conducting solid polymer electrolytes: advances and perspectives, *Chem. Soc. Rev.*, 2017, **46**, 797–815.
3 R. Meziane, J.-P. Bonnet, M. Courty, K. Djellab and M. Armand, Single-ion polymer electrolytes based on a delocalized polyanion for lithium batteries, *Electrochim. Acta*, 2011, **57**, 14–19.
4 E. Glynos, P. Petropoulou, E. Mygiakis, A. D. Nega, W. Pan, L. Papoutsakis, E. P. Giannelis, G. Sakellariou and S. H. Anastasiadis, Leveraging Molecular Architecture To Design New, All-Polymer Solid Electrolytes with Simultaneous Enhancement in Modulus and Ionic Conductivity, *Macromolecules*, 2018, **51**, 2542–2550.
5 E. Glynos, L. Papoutsakis, W. Pan, E. P. Giannelis, A. D. Nega, E. Mygiakis, G. Sakellariou and S. H. Anastasiadis, Nanostructured Polymer Particles as Additives for High Conductivity, High Modulus Solis Polymer Electrolytes, *Macromolecules*, 2017, **50**, 4699–4706.
6 E. Glynos, C. Pantazidis and G. Sakellariou, Designing All-Polymer Nanostructured Solid Electrolytes: Advances and Prospects, *ACS Omega*, 2020, **5**, 2531–2540.
7 K. Y. Mya, K. P. Pramoda and C. B. He, Crystallization behavior of star-shaped poly(ethylene oxide) with cubic silsesquioxane (CSSQ) core, *Polymer*, 2006, **47**, 5035–5043.
8 P. F. Cao, Z. Wojnarowska, T. Hong, B. Carroll, B. Li, H. Feng, L. Parsons, W. Wang, B. S. Lokitz, S. Cheng, V. Bocharova, A. P. Sokolov and T. Saito, A star-shaped

single lithium-ion conducting copolymer by grafting a POSS nanoparticle, *Polymer*, 2017, **124**, 117–127.

9 E. Harth, B. Van Horn, V. Y. Lee, D. S. Germack, C. P. Gonzales, R. D. Miller and C. J. Hawker, A Facile Approach to Architecturally Defined Nanoparticles via Intramolecular Chain Collapse, *J. Am. Chem. Soc.*, 2002, **124**, 8653–8660.

10 H. Gao and K. Matyjaszewski, Synthesis of functional polymers with controlled architecture by CRP of monomers in the presence of cross-linkers: From stars to gels, *Prog. Polym. Sci.*, 2009, **34**, 317–350.

11 J. M. Ren, T. G. McKenzie, Q. Fu, E. H. H. Wong, J. Xu, Z. An, S. Shanmugam, T. P. Davis, C. Boyer and G. G. Qiao, Star Polymers, *Chem. Rev.*, 2016, **116**, 6743–6836.

12 C. Pantazidis, S. Andreou, E. Glynos and G. Sakellariou, Synthesis of a well-defined polyelectrolyte by controlled/"living" nitroxide-mediated radical polymerization. Kinetic study, *Eur. Polym. J.*, 2020, **134**, 109815.

13 J.-F. Lutz, P. Lacroix-Desmazes and B. Boutevin, The Persistent Radical Effect in Nitroxide Mediated Polymerization: Experimental Validity, *Macromol. Rapid Commun.*, 2001, **22**, 189–193.

14 D. A. Shipp and K. Matyjaszewski, Kinetic Analysis of Controlled/"Living" Radical Polymerizations by Simulations. 1. The Importance of Diffusion-Controlled Reactions, *Macromolecules*, 1999, **32**, 2948–2955.

15 F. Chauvin, P.-E. Dufils, D. Gigmes, Y. Guillaneuf, S. R. A. Marque, P. Tordo and D. Bertin, Nitroxide-Mediated Polymerization: The Pivotal Role of the k_d Value of the Initiating Alkoxyamine and the Importance of the Experimental Conditions, *Macromolecules*, 2006, **39**, 5238–5250.

16 Z. Xue, D. He and X. Xie, Poly(ethylene oxide)-based electrolytes for lithium-ion batteries, *J. Mater. Chem. A*, 2015, **3**, 19218–19253.

17 E. Núñez, C. Ferrando, E. Malmström, H. Claesson, P. E. Werner and U. W. Gedde, Crystal structure, melting behavior and equilibrium melting point of star polyesters with crystallizable poly(ε-caprolactone) arms, *Polymer*, 2004, **45**, 5251–5263.

18 S. Coppola, N. Grizzuti, G. Floudas and D. Vlassopoulos, Viscoelasticity and crystallization of poly(ethylene oxide) star polymers of varying arm number and size, *J. Rheol.*, 2007, **51**, 1007.

19 J. Baschnagel, D. Cangialosi, K. Fukao, E. Glynos, L. M. C. Janssen, M. Müller, M. Muthukumar, U. Steiner, J. Xu, S. Napolitano and G. Reiter, Processing pathways decide polymer properties at the molecular level, *Macromolecules*, 7146, **2019**, 52.

20 A. A. Rojas, S. Inceoglu, N. G. Mackay, J. L. Thelen, D. Devaux, G. M. Stone and N. P. Balsara, Effect of Lithium-Ion Concentration on Morphology and Ion Transport in Single-Ion-Conducting Block Copolymer Electrolytes, *Macromolecules*, 2015, **48**, 6589–6595.

21 S. Lascaud, M. Perrier, A. Vallee, S. Besner, J. Prud'homme and M. Armand, Phase Diagrams and Conductivity Behavior of Poly(ethylene oxide)-Molten Salt Rubbery Electrolytes, *Macromolecules*, 1994, **27**, 7469–7477.

22 J. L. Thelen, S. Inceoglu, N. R. Venkatesan, N. G. Mackay and N. P. Balsara, Relationship between Ion Dissociation, Melt Morphology, and Electrochemical Performance of Lithium and Magnesium Single-Ion Conducting Block Copolymers, *Macromolecules*, 2016, **49**, 9139–9147.

23 A. Chremos, E. Glynos and P. F. Green, Structure and dynamical intra-molecular heterogeneity of star polymer melts above glass transition temperature, *J. Chem. Phys.*, 2015, **142**, 044901.

24 P. Bacova, E. Glynos, S. H. Anastasiadis and V. Harmandaris, Spatio-temporal heterogeneities in nano-segregated single-molecule polymeric nanoparticles, *Soft Matter*, 4584, **2020**, 16.

25 T. Pakula, D. Vlassopoulos, G. Fytas and J. Roovers, Structure and Dynamics of Melts of Multiarm Polymer Stars, *Macromolecules*, 8931, **1998**, 31.